İSTANBUL UNIVERSITY CERRAHPAŞA

ORIGINAL ARTICLE
Electrica 2024; 24(2): 477-488

Implementing Coati Optimization Algorithm in Fuzzy Logic-Based Fractional-Order Tilt-Integral-Derivative Controller for Automatic Generation Control in Multi-Area Multi-Unit Power System

Debashis Sitikantha[1], Binod Kumar Sahu[2], Debiprasanna Das[2]

[1]Department of Electrical and Electronics Engineering, Institute of Technical Education and Research, Siksha 'O' Anusandhan Deemed to be University, Bhubaneswar, Odisha, India
[2]Department of Electrical Engineering, Institute of Technical Education and Research, Siksha 'O' Anusandhan Deemed to be University, Bhubaneswar, Odisha, India

Cite this article as: D. Sitikantha, B. Kumar Sahu and D. Das, "Implementing coati optimization algorithm in fuzzy logic based fractional-order tilt-integral-derivative controller for automatic generation control in multi-area multi-unit power system," *Electrica*, 24(2), 477-488, 2024.

ABSTRACT

When there is a mismatch in electrical power produced and the demanded electrical loading in an interconnected electrical power system, it results in deviations in frequencies in the constituent areas and in tie-line power as well. This issue is addressed by automatic generation control which when coupled with intelligent controller leads to fast recovery of the deviations both in tie-line power and frequencies from the assigned ranges associated with each of these areas. This paper is an attempt to utilize fuzzy logic-based fractional-order tilt-integral-derivative (Fuzzy FOTID) controller with gains/parameter optimized using the recent Coati Optimization Algorithm. Comparative studies are undertaken as a part of this work to exhibit the Fuzzy FOTID controller's supremacy over other popular controllers like proportional-integral-derivative, TID, and FOTID.

***Index Terms*—**AGC, area control error (ACE), fuzzy FOTID, Coati optimization algorithm (COA), robustness

I. INTRODUCTION

The human races' pursuit for energy is endless. Out of all the forms of energy, electrical energy is the most convenient, flexible form of energy. Hence the demand for electrical energy always follows a rising curve. Due to this, the complexity and the vastness of the electrical power system (EPS) is increasing. The incorporation of wide variety of generation systems in the interconnected EPS, makes it venerable and sensitive to load surges. Maintaining equilibrium among the generation of electrical power and the demand plus the losses is a herculean task. Any disturbance like a sudden surge/drop of load, generating unit failure or a fault in the system jeopardies this balance leading to deviation of frequencies and tie-bus power from its prescribed range and specified tolerance limits, respectively. This in turn affects the frequency dependent loads adversely and may also lead to large-scale system instability [1]. The automatic generation control (AGC) maintains this equilibrium between production/generation and variation in loading conditions. The AGC has the major goal to regulate/maintain the frequency within the designated range while facilitating power exchanges between control areas at the contracted values. This action is usually referred as load frequency control (LFC) [2].

In order to maintain stability and carry on a seamless operation of the EPS it becomes necessary to maintain a null steady-state error in the tie-bus power aberrations amid area frequencies. Researchers worldwide have put their effort in developing and designing various controllers and controlling strategies for the controller as it plays a substantial role in achieving the above objective. Proportional-integral-derivative (PID) controllers [3], by far are popularly employed for AGC in regards to their simple architecture and implementation. A study regarding the implementation of PID controller for LFC using Hybrid for multi-source power systems [4] proves the efficacy of PID controllers when tuned with intelligent optimization algorithms. Integral (I), proportional-integral (P-I), integral-derivative (I-D) controllers were extensively studied by researchers/engineers globally to develop control strategies for the AGC [5] due to their modest architecture and ease of applicability. In [6], design and performance analysis of controllers like fuzzy-based PI

Corresponding author:
Binod Kumar Sahu

E-mail:
binoditer@gmail.com

Received: September 16, 2023

Revision Requested: November 1, 2023

Last Revision Received: March 4, 2024

Accepted: April 12, 2024

Publication Date: May 31, 2024

DOI: 10.5152/electrica.2024.23145

and PID using Bacterial Foraging Optimization Algorithm for AGC of multi-area interconnected traditional and restructured EPS was presented. When classical controllers incorporated with fuzzy logic control (FLC) are used in AGC, it proves to be giving superior dynamic responses than non-fuzzy-based controllers [7-8]. Tilt-integral-derivative (TID) controller [9] has an architecture alike conventional PID controller with the exception that the proportional gain is substituted by a tilted proportional gain $s^{\left(\frac{-1}{n}\right)}$. The TID controller has advantages of an easier tuning, better rejection of disturbances and better immunity to system parameter variations along with higher degree of freedom for controller parameters. Tilt-integral-derivative controller has higher degree of freedom in choosing control parameters [10-11]. In recent times, researchers have shifted their focus on fractional-order (FO) controllers. Fractional order controllers are based on fractional differential equations and when Laplace transformation is applied, the transfer function thus obtained, helps in designing the controller [10, 12]. Fractional-order controllers have more parameters for tuning than conventional controllers, thus helps in better performance. However, to achieve faster system dynamics and minimize ACE at the earliest, in an environment of uncertainties and parameter variations, conventional and FO controllers are incorporating with FLC. Controllers like FO-cascaded-fuzzy PI-FOPID, fuzzy-FO integral-derivative with ultra capacitor energy storage system and optimal cascade-fuzzy-FO integral-derivative with filter used for 2-area thermal and hydro-thermal power plants with gains/parameters of controller tuned by stochastic Imperialist Competitive Algorithm (ICA) have been discussed in detail in Arya [13-15]. In [16], cascaded fractional order proportional derivative (FOPD)n-fractional order proportional integral derivative (FOPID)n controller has been used for a 3-area EPS, with each area comprising of thermal-dish stirling solar thermal system (DSTS). The controller's parameters are augmented by Crow Search Algorithm (CSA) using hybrid peak area-Integral squared error (HPA-ISE) as the performance index. The investigation was carried out in real time (RT) lab with the areas integrated using high voltage direct current (HVDC) links.

The right selection of meta-heuristic optimization tool to tune up the gains/parameters of FLC-based FO controllers is very important. The right choice ensures fast response and minimum deviations. Computational techniques such as Particle Swarm Optimization [3], Hybrid Particle Swarm Optimization (PSO) [8], Pathfinder Algorithm [11], ICA [13-15], CSA [16], Genetic Algorithm [17], Teaching–Learning-Based Optimization (TLBO) [18], Grasshopper Optimization Algorithm [19], Whale Optimization Algorithm (WOA) [20] Salp Swarm Algorithm (SSA) [21] are widely employed for tuning the controllers' gain and scaling factor.

In this article an attempt is carried out to make use of the Coati Optimization Algorithm (COA) [20] to tune up the various gains/parameters for the fuzzy FOTID controller. This is an upcoming bio-inspired metaheuristic optimization method developed by Mohammad Dehghani et al. [22] in the year 2022.

Here in this paper, Fuzzy FOTID-based controller is designed and used for the LFC problem in a two-area, six-unit hydro-thermal-gas-b ased PS. The gains, scaling factors are tuned by COA. The objective function used is the "Integral Time Absolute Error" (ITAE).

This study's major contributions are as follows:

a. Designing and modeling a two-area, six-unit hydro-thermal-gas-based PS including its associated nonlinearities namely the Generation Rate Constant (GRC) and Governor Dead Band (GDB) in SIMULINK/MATLAB R2020a using *i*5 and 64-bit processor with 8GB DDR4, RAM.
b. Model proposed employs a PID, TID, FOTID, fuzzy PID, fuzzy TID, and fuzzy FOTID.
c. Coati optimization algorithm is used in optimizing the gains/parameters and scaling factors of the proposed controllers.
d. Model proposed is subjected to stability analysis in frequency domain (Bode plot).
e. Sporadic load variation (in the form of step input) is introduced in Area_1, for robustness verification of the controller, fuzzy FOTID.

The entire study can be segregated into a number of different sections. Section 1 presents introduction and survey of the literatures followed by, Section 2 describes the PS considered in the work, Section 3 introduces the controller proposed, Section 4 talks about optimization technique used, Section 5 discusses about simulation results and their interpretations whereas Section 6 writes about the conclusion for the work undertaken.

II. POWER SYSTEM INVESTIGATED

The PS examined is a two-area, six-unit PS having a reheat-type thermal, hydro, gas turbine-based electrical power plant unit per area. The non-linearities associated with each unit in each area is taken into consideration for a more realistic approach. The block diagram is shown in Fig. 1 [11, 20]. Participation factor of the power plants under consideration is 0.5. Governor Dead Band for hydro and thermal power plant are respectively taken as +0.05% and +0.06%. Similarly, GRC for thermal generators and hydro generators is +3% and +6% p.u./s, respectively. N_1 and N_2 are the Fourier series coefficients of governor's deadband and are taken as 0.8 and −0.2 respectively for a dead band corresponding to ±0.05% and $\omega_0 = \pi$ with an assumption that the sinusoidal oscillation has a time period $T_0 = 2$ seconds.

***Nomenclature*:**

R_G, R_H, R_T	Speed regulation parameter constants of governor for gas, hydro, thermal units, respectively (in Hz/p.u. MW)
B	Frequency bias factor (in p.u. MW/Hz)
T_{GT}, T_{GH}	Speed governor time constants of thermal, hydro units respectively (in seconds)
T_R	Reheater time constant (in seconds)
T_T	Reheat type steam turbine time constant (in seconds)
K_R	Reheat steam turbine constant
K_1, K_{11}	FLC input scaling factor of controller 1
K_2, K_{22}	FLC input scaling factor of controller 2
T_{RS}	Governor reset time (in seconds)
T_{RH}	Speed governor transient droop time of hydro turbine (in seconds)
T_W	Starting time of penstock water for hydro plant (in seconds)
c_G	Valve positioner of gas turbine
b_G	Gas turbine constant
X_G	Lead time constant of gas turbine speed governor (in seconds)
Y_G	Lag time constant of gas turbine speed governor (in seconds)

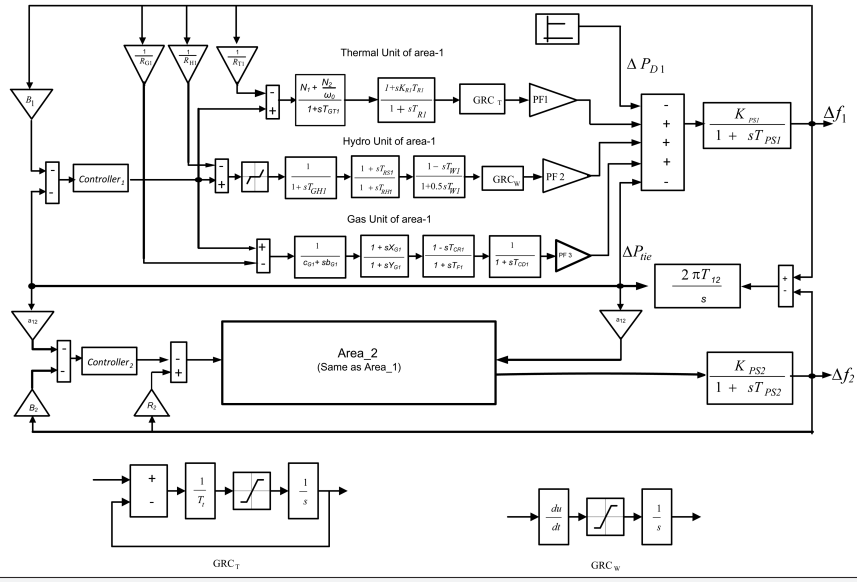

Fig. 1. Block diagram representation of two-area power system having hydro-thermal-gas power plants.

***Nomenclature*:**	
T_{CR}	Combustion time delay for gas turbine (in seconds)
T_F	Fuel time constant for gas turbine (in seconds)
T_{CD}	Discharge time constant for gas turbine compressor (in seconds)
$K_{P.S.}$	Gain of the PS (in Hz/p.u. MW)
$T_{P.S.}$	Time constant of the PS (in seconds)
T_{12}	Synchronization coefficient amid Area_1 and Area_2 (in p.u. MW/Hz)
PF	Participation factor
Δf	Frequency deviation (in Hz)
ΔP_D	Change in load demand (in p.u. MW)
ΔP_{tie}	Deviation in tie-line power (in p.u. MW)

III. PROPOSED CONTROLLER DESCRIPTIONS

A. Proportional-Integral-Derivative Controller

Proportional-integral-derivative controller has extensive usage in industries because it is simple in its structure and implementation. It has three operational modes: proportional (P), integral (I) and derivative (D) mode. It can be self-tuned for reducing the error in process plant output. Proportional-integral-derivative controller's output in time domain (TD) is mathematically described by equation 1 as:

$$u(t)=K_{\_P}.e(t)+K_{\_I}.\int_0^t e(t)dt+K_{\_D}.\frac{de(t)}{dt} \quad (1)$$

where $K_{\_P}$, $K_{\_I}$, and $K_{\_D}$ are the proportional, integral, and derivative gains, respectively; u (t) is the output of controller; and e (t) is the error input.

$$\mathrm{ACE}(t)=B.\Delta f(t)+\Delta P_{tie} \quad (2)$$

B. Tilt-Integral-Derivative Controller

Tilt-integral-derivative controller is almost same in its structure to that of the PID controller except that the proportional action is modified by tilt-proportional action due to the presence of $\frac{1}{\frac{1}{s^n}}$ transfer block, where n is a real and non-zero number. Due to this, parameter n gets included along with $K_{\_P}$, $K_{\_I}$, and $K_{\_D}$ that aids in better tuneability, noise rejection and also makes the system more immune to parameter variations [11]. The output of TID controller in TD is mathematically described by equation 3 as:

$$u(t)=\left(\frac{K_{\_P}}{\frac{1}{s^n}}+\frac{K_{\_I}}{s}+sK_{\_D}\right).e(t) \quad (3)$$

C. Fractional-Order Tilt-Integral-Derivative Controller

Over some years FO controllers have gained a lot of popularity among the researchers engaged in the area of LFC/AGC owing to their greater degree of freedom in tuning, that results in extended range of stability and more flexibility. In this study the concept of FO is incorporated in TID controller to harness the advantage of both. The architecture of FOTID controller is as illustrated in Fig. 2.

The architecture of a FOTID controller is almost same as that of a TID controller with the exception that instead of the integrator and

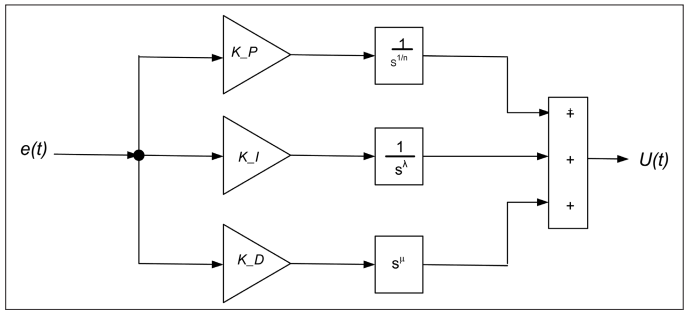

Fig. 2. Structure of Fractional-Order Tilt-Integral-Derivative Controller.

differentiator block FO integrator and differentiator block is used. The TD transfer function of FOTID controller is mathematically represented in equation (4).

$$u(t)=\left(\frac{K_{\_P}}{\frac{1}{s^{n}}}+\frac{K_{\_I}}{s^{\lambda}}+s^{\mu}.K_{\_D}\right).e(t) \tag{4}$$

where μ and λ are respectively the fractional/non-integer derivative order and fractional/non-integer integrator order.

D. Fuzzy Fractional-Order Tilt-Integral-Derivative Controller

The structure of a fuzzy-FOTID controller is presented in Fig. 3. Fuzzy logic control uses the ability of humans' vague assessments by mimicking the human reasoning and decision making that results in a greater number of outcomes. The FLC basically has a fuzzifier, an inference-engine, a defuzzifier, fuzzy rule-base, and membership functions as illustrated in Fig. 4 showing the input and the output. The "Centre of gravity" method is executed in obtaining output in crisp form. Table I presents the rule-base.

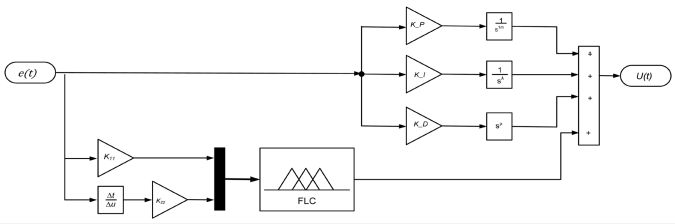

Fig. 3. Structure of fuzzy-fractional-order tilt-integral-derivative controller.

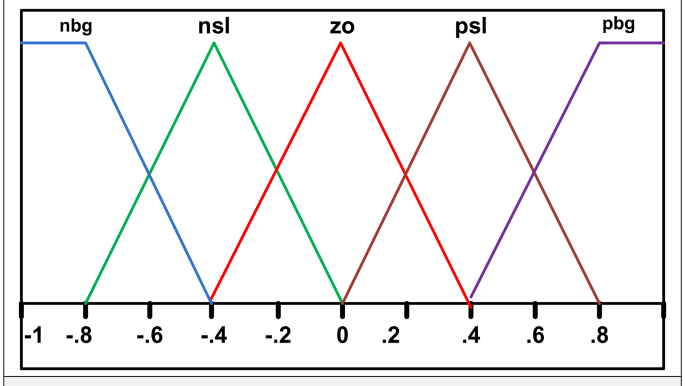

Fig. 4. Membership function.

TABLE I. RULE-BASE FOR FLC-BASED CONTROLLER

de/dt ⟶ e↓	nbg	nsl	z0	psl	pbg
nbg	nbg	nbg	nsl	nsl	z0
nsl	nbg	nsl	nsl	z0	psl
z0	nsl	nsl	z0	psl	psl
psl	nsl	z0	psl	psl	pbg
pbg	z0	psl	psl	pbg	pbg

IV. OPTIMIZATION ALGORITHM ADOPTED

A very recent optimization algorithm tool by the name of COA developed by Mohammad Dehghani et al. [22] is utilized here. It is a population-based bio inspired metaheuristic optimization algorithm. Its basis is the modeling of the natural behavior of coatis that involves their application of smart strategies during hunting of their prey iguana as well as strategy while facing and fleeing from their predators. These two strategies form the main inspiration behind this new optimization algorithm.

A. Initialization

The coatis are considered as the population members. The search region that gives the values of the decision variables are the positions of individual coati in the search area. In this stage the positions of each coati are randomly generated in the search area matrix also called the population matrix [*X*] of the order [*N X D*]. Mathematically,

$$X_j \equiv x_{i,j} = lb_j + rand.\left(ub_j - lb_j\right) \tag{5}$$

where X_j is the "*i*"th coati's position in the search area

$x_{i,j}$ is the value of "*j*"th coati in the search area

N is the number of coatis

D is the number of decision variables

rand is a random real number in a range of [0, 1]

ub_j, lb_j are the upper, lower limits of the "*j*"—th decision variable

$$\text{and } \left[X\right] = \begin{matrix} X_1 \\ \vdots \\ X_{N\,NX1} \end{matrix} = \begin{bmatrix} x_{1,1} & \cdots & x_{1,D} \\ \vdots & \ddots & \vdots \\ x_{N,1} & \cdots & x_{N,D} \end{bmatrix}_{NXD} \tag{6}$$

B. Updating

The objective function's numerical value gives the fitness of the candidate solution. The fittest member is considered the best member. With subsequent iterations the fittest members are updated and only the best population appears at the end of the iteration cycle.

The objective function values are defined as:

$$\left[ITAE\right] = \begin{matrix} ITAE_1 \\ \vdots \\ ITAE_N \end{matrix} = \begin{matrix} ITAE\left(X_1\right) \\ \vdots \\ ITAE\left(X_N\right) \end{matrix} \tag{7}$$

The updating involves updating the position of the coatis that is based on two separate strategies followed by the coatis during (i) when attacking their prey i.e., the iguanas and (ii) when escaping from their predators. The first strategy is called the exploration phase and the second one is exploitation phase.

C. Exploration Phase

This phase involves the hunting and attacking strategy for the iguanas. For hunting, a half of the group of coatis climb on to the tree to frighten up the iguanas while rest part of the group waits down under the tree for the iguana to tumble down from the tree. Once the iguana falls on the ground the grounded group of coatis move toward the prey, attacks and hunts it. The position of the coati nearest to the iguana is considered to be the best among the population.

Since half the coatis' population ascend the tree to scare iguana, it can be mathematically modeled as follows:

$$X_i^{P1} \equiv x_{i,j}^{p1} = x_{i,j} + rand.\left(iguana_j - I.x_{i,j}\right) \quad (8)$$

where X_i^{P1} is the "*i*"th coati's calculated new position

$x_{i,j}^{p1}$ is the "*i*"th coati's calculated new position in the "*j*"th dimension

$i = 1, 2, \ldots\ldots \left(N/2\right)$

$j = 1, 2, \ldots\ldots D$

I = Integer {1,2}

rand is a random real number in a range of [0, 1]

$iguana_j$ is the position of best member

When the iguana tumbles down the ground at any random location in the search area, the grounded group of coatis move towards it in the search region. Mathematically it is modeled as under.

$$iguana_j^g = lb_j + rand.\left(ub_j - lb_j\right) \quad (9)$$

$$X_i^{P1} \equiv x_{i,j}^{p1} = \begin{cases} x_{i,j} + rand.\left(iguana_j^g - I.x_{i,j}\right), ITAE_{iguana}^g < ITAE_i \\ x_{i,j} + rand.\left(x_{i,j} - iguana_j^g\right), else \end{cases} \quad (10)$$

where $i = \left(N/2\right)+1, \left(N/2\right)+2, \cdots \left(N/2\right)+N$ (11)

j=1, 2, ……*D*

$iguana_j^g$ is the position of iguana on ground

Once new position of each coati is evaluated and updated in the population matrix a comparison is done between the old values and new values of the objective function. Mathematically it can be stated as under equation (12).

$$X_i = \begin{cases} X_i^{p1}, ITAE_i^{p1} < ITAE_i \\ X_i, else \end{cases} \quad (12)$$

where $ITAE_i^{p1}$ is the value of $ITAE\left(x_{i,j}^{p1}\right)$

D. Exploitation Phase

This phase mimics the natural behavior of coatis while escaping from their predators. This phase involves updating of coatis' position in the search area when escaping from their predators by moving on to a safer position closer to its current position.

For simulating this behavior, a new position near this current coati position is randomly generated as determined by equations from (13), (14), and (15).

$$lb_j^{loc} = \frac{lb_j}{t} \quad (13)$$

$$ub_j^{loc} = \frac{ub_j}{t} \quad (14)$$

$$X_i^{P2} \equiv x_{i,j}^{p2} = x_{i,j} + \left(1 - 2.rand\right).\{(lb_j^{loc} + rand.\left(ub_j^{loc} - lb_j^{loc}\right)\} \quad (15)$$

where $i = 1, 2, \ldots\ldots\ldots N$

$j = 1, 2, \ldots\ldots\ldots D$

t is the number of iterations, 1, 2, … t

lb_j^{loc}, ub_j^{loc} are the lower, upper local bound respectively of the "*j*"th decision variable.

E. Termination

The new position values thus calculated is accepted if there is improvement in the objective function values as given in equation (16).

$$X_i = \begin{cases} X_i^{p2}, ITAE_i^{p2} < ITAE_i \\ X_i, else \end{cases} \quad (16)$$

where X_i^{p2} is the "*i*"th coati's calculated new position during phase 2.

On the basis of the first and second phases, once all the coati position in the search area is updated, as per equations (5) to (16), the iteration of the COA is complete. After all the iterations are completed, the COA returns the best solution as the output. The pseudo code for COA is presented below. The flowchart is given in Fig. 5.

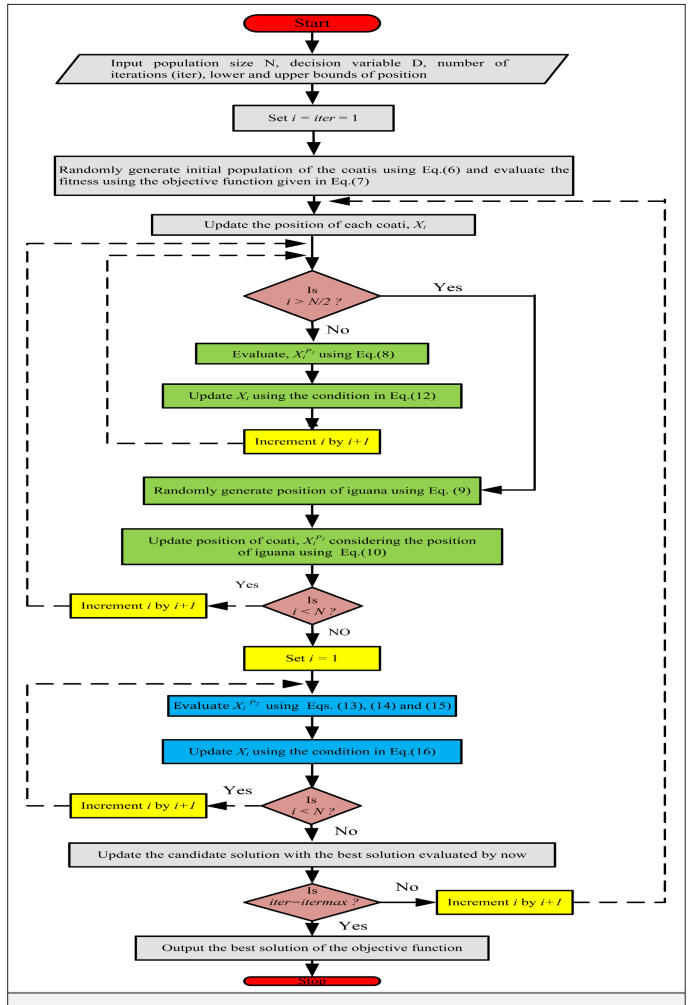

Fig. 5. Flowchart for Coati Optimization Algorithm.

Start COA

Declare the objective function.

Set the size of population (*N*), number of decision variables, (*D*) and the maximum iteration number (*itermax*).

Evaluate the positions of all the coatis by random generation using equation (5) and then evaluate the objective function for this initial position.

For *iter* = 1: *itermax*

Update the position of the iguana on the basis of position of the best member in the population.

Phase 1: Exploration Phase

For $i = 1: (N/2)$

Evaluate the new position of i^{th} coati using Eq. (8).

Update the position of the i^{th} coati using Eq. (12).

End of for loop

For $i = 1 + (N/2) : N$

Evaluate randomly the position for the iguana using Eq. (9).

Evaluate the position of the i^{th} coati using Eq. (10).

Update the position of the i^{th} coati using Eq. (12).

End of for loop

Phase 2: Exploitation Phase

Evaluate the lower and upper bounds for the variables using Eq. (13) and (14).

For $i = 1: N$

Evaluate the new position for the i^{th} coati using Eq. (15).

Update the position of the i^{th} coati using Eq. (16).

End of for loop

Update the solution with the best solution found by now.

End of for loop

Output the best solutions processed by using COA for the given problem.

End COA

The choice for implementing COA was made after considering the simulation studies and results presented in [22]. Metrics like search history, updation trajectory of first member in first dimension, mean fitness of coati population, and convergence curve were compared for a number of benchmark functions with the yardstick like mean/average, standard deviation, rank and computational time among some popular optimization algorithms like WOA, PSO, and TLBO to name a few. Coati Optimization Algorithm shows high capability in scanning the search region for global and local levels, thereby facilitating early convergence towards optimal solution. The computational complexities of COA predominantly revolve around four factors namely (a) population size (*N*), (b) number of decision variables (*D*), (c) number of iterations (*iter*) and (d) objective function (*ITAE*). It is exactly what is demanded during the optimization to tune up the proposed controller. So, in this work, COA is written in MATLAB .m file and the Simulink model is called by the COA program for optimizing the gain parameters and scaling factors of the Fuzzy FOTID controller.

Benchmark functions are widely used as performance indicators for metaheuristic algorithms. Metaheuristic algorithms that show good

TABLE II. BENCHMARK FUNCTION

Optimization Algorithm	Benchmark Function	Optimum Value	Min. Value	Max. Value	Mean Value	Std. Dev.	Evaluation Time (in Seconds)
COA	Ackley	0	8.8818×10^{-6}	8.8818×10^{-6}	8.8818×10^{-6}	0	0.0547
SSA			5.6695×10^{-5}	6.6678×10^{-4}	9.4452×10^{-5}	0	0.1257
PSO			8.6324×10^{-5}	5.3529×10^{-4}	3.2361×10^{-5}	5.6629×10^{-12}	0.0126
COA	Beale	0	9.5×10^{-16}	0.1027×10^{-6}	0.0013×10^{-6}	0.0103×10^{-6}	0.0330
SSA			1.1911×10^{-14}	7.3256×10^{-6}	0.0572×10^{-6}	6.2539×10^{-6}	0.0785
PSO			1.9502×10^{-13}	5.6325×10^{-5}	5.2587×10^{-6}	0.8956×10^{-5}	0.0183
COA	Cross in Tray	−2.0626	−2.0626	−2.0626	−2.0626	3.1689×10^{-10}	0.0373
SSA			−2.0626	−2.0626	−2.0626	5.6283×10^{-9}	0.0576
PSO			−2.0626	−2.0626	−2.0626	3.3897×10^{-7}	0.0153
COA	Colville	0	0.0101×10^{-8}	0.3193×10^{-6}	0.0829×10^{-7}	0.0705×10^{-5}	0.0272
SSA			0.5679×10^{-8}	3.5629×10^{-6}	0.2589×10^{-7}	1.2375×10^{-6}	0.0837
PSO			5.2967×10^{-7}	3.6928×10^{-4}	3.2687×10^{-6}	2.3668×10^{-6}	0.0086

COA, Coati Optimization Algorithm; PSO, Particle Swarm Optimization; SSA, Salp Swarm Algorithm.

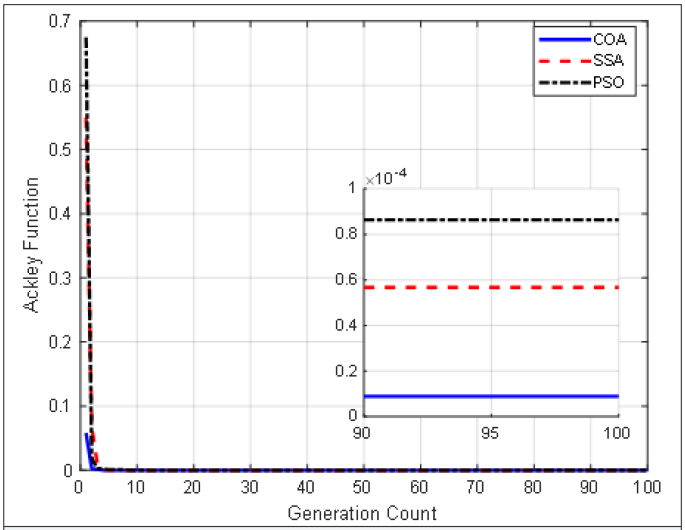

Fig. 6. Convergence characteristics of Ackley function.

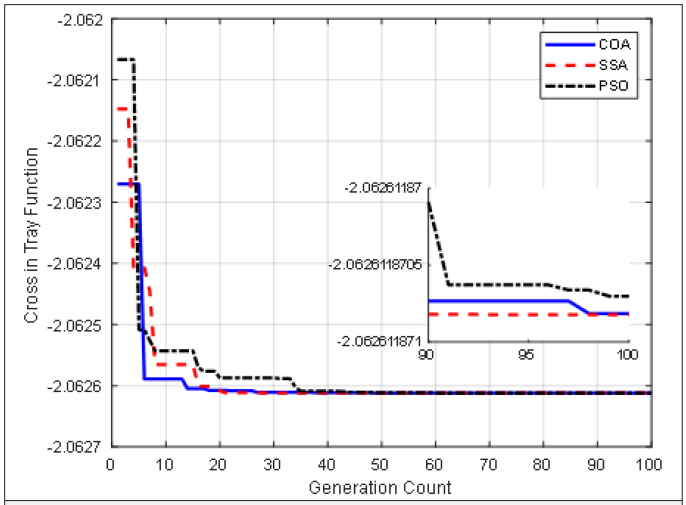

Fig. 8. Convergence characteristics of Cross in Tray function.

results on these functions, perform well to solve real-world optimization problems. The COA is subjected to a set of benchmark function tests to prove its efficiency and convergence which includes Ackley, Beale, Cross in Tray, and Colville functions. A comparison in performance considering minimum (min.), maximum (max.), average/mean values, standard deviation (std. dev.) and evaluation time (in seconds) is also done with the results obtained by employing the SSA and PSO. The results are tabulated as in Table II and illustrated in figures from Figs. 6–9. The results clearly show the performance of COA has an edge over the two algorithms considered in terms of performance and computational time.

V. SIMULATION RESULTS AND THEIR INTERPRETATIONS

A. Analysis of Transient Performances

The AGC system proposed in this paper is modeled and simulated in MATLAB/Simulink (Version R2020a). Model taken is a multi-area, multi-unit EPS with two areas and six units. Each of these areas consists of a hydro, thermal and gas-based generating power plant.

Here the non-linearities like GDB and GRC associated with each generating plants is considered for a realistic analysis. The numerical values of GRC and GDC along with all the system parameters are the ones presented in Appendix and Section 2. Non-fuzzy-based controllers have their gains within the range [0, 2] and that of fuzzy FOTID in [0, 0.1]. In this research COA is used to optimize the gain parameters. For the optimization, ITAE is taken as the cost/objective function. Fuzzy logic is embedded in FOTID controller to make it behave as an intelligent controller. The optimization is carried out with size of population and number of iterations both equal to 100. Table III tabulates the gains, tuned parameters, and scaling factors of the different controllers after optimization with due consideration to the non-linearities in the system. A perturbation of 0.1 p.u. in the form of a step load input is introduced to the test model during simulation for analyzing the dynamic behavior of the test systems.

The dynamic response of frequency and tie-line power deviations with respect to time is illustrated in Fig. 10 through Fig. 12. The transient performance indicators are tabulated in Table IV.

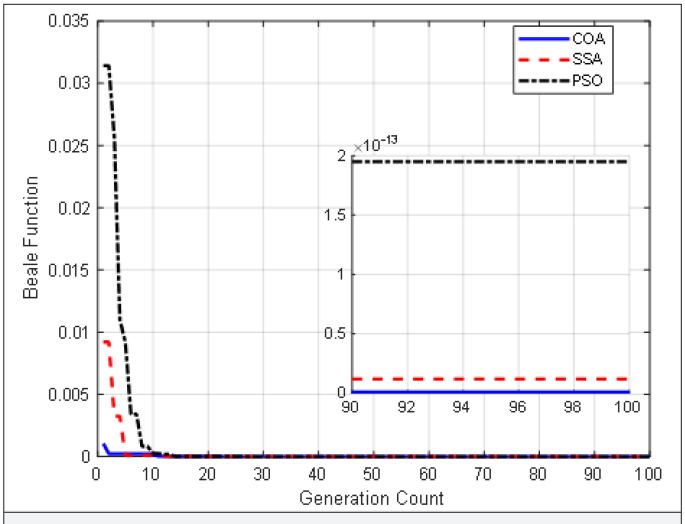

Fig. 7. Convergence characteristics of Beale function.

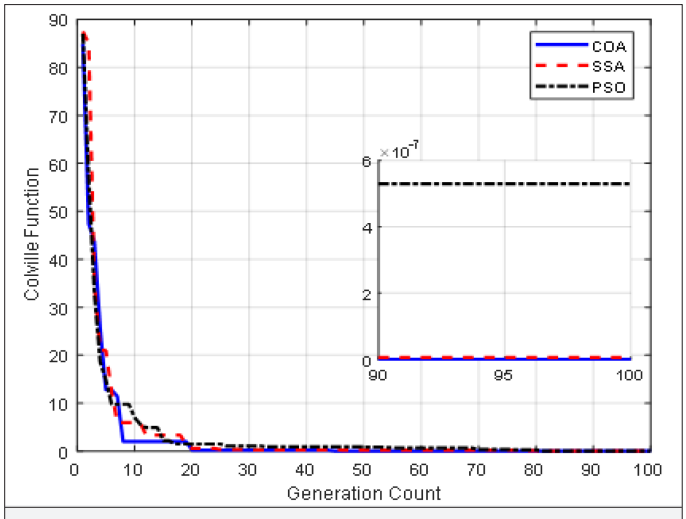

Fig. 9. Convergence characteristics of Colville function.

TABLE III. CONTROLLER GAIN/PARAMETER/SCALING FACTOR

Gain/Parameter/Scaling Factor of Fuzzy Fractional-Order Tilt-Integral-Derivative Controller							
Area_1				**Area_2**			
$K_{\_P1}$	$K_{\_i1}$	$K_{\_D1}$	n_1	$K_{\_P2}$	$K_{\_i2}$	$K_{\_D2}$	n_2
0.8761	1.0167	1.3466	0.8621	0.1000	0.7558	0.2510	0.9627
λ_1	μ_1	K_1	K_{11}	λ_2	μ_2	K_2	K_{22}
0.3363	0.9320	0.6546	0.7621	0.5438	0.5101	0.0100	0.8289
Gain/Parameter of Fractional-Order Tilt-Integral-Derivative Controller							
Area_1				**Area_2**			
$K_{\_P1}$	$K_{\_i1}$	$K_{\_D1}$	n_1	$K_{\_P2}$	$K_{\_i2}$	$K_{\_D2}$	n_2
0.1000	0.6990	1.8806	2.000	0.5827	0.5815	0.6985	2.1163
λ_1		μ_1		λ_2		μ_2	
0.9051		0.9892		0		0.5832	
Gain/Parameter of Tilt-Integral-Derivative Controller							
Area_1				**Area_2**			
$K_{\_P1}$	$K_{\_i1}$	$K_{\_D1}$	n_1	$K_{\_P2}$	$K_{\_i2}$	$K_{\_D2}$	n_2
1.3838	0.0502	1.2716	0.9986	0.8841	0.1123	1.4987	1.3939
Gain of Proportional-Integral-Derivative Controller							
Area_1					**Area_2**		
$K_{\_P1}$	$K_{\_i1}$	$K_{\_D1}$	$K_{\_P2}$	$K_{\_i2}$	$K_{\_D2}$		
1.4958	0.1496	1.4214	0.1051	1.0660	1.4975		

In the figures shown from Fig. 10, Fig.11 and Fig. 12, a comparison analysis of the responses for PID, TID, FOTID and Fuzzy FOTID controllers between the frequency deviations versus time and tie-line power deviations versus time in Area_1 and Area_2 is illustrated. Though among all of these responses the PID controllers having the minimum overshoot and in many of the responses the undershoot is also better, yet the settling time is seen to be the highest among all. The TID controllers though are capable in leading to a better settling time response but the overshoot and undershoots are not impressive. But when the TID controller is coupled with a FO operator to form a FOTID controller the performance is greatly improved. The undershoot and the overshoot of TID controller drastically improved with the introduction of FO operator and the undershoot and the overshoot reduced along with the settling time. The proposed controller, Fuzzy FOTID, which is FOTID controller embedded with a FLC gives the best responses among all the other controllers. The overshoot and undershoot are among the best and the settling time is the minimum among all. It can also be noted that there is practically no oscillation in the responses.

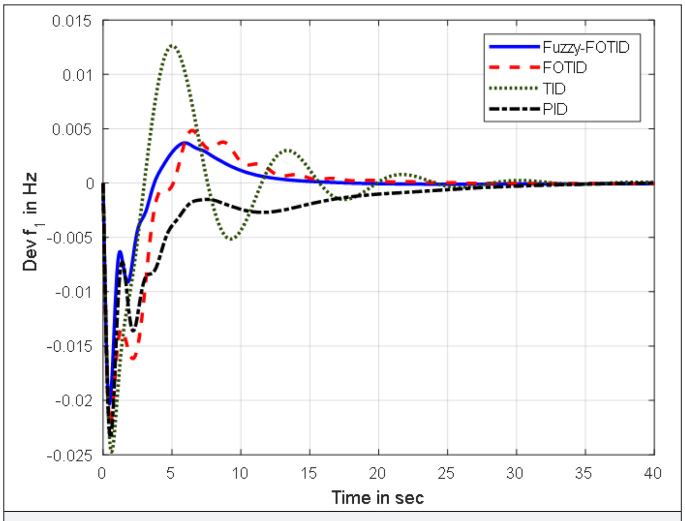

Fig. 10. Area_1 Frequency deviation w.r.t time.

B. Stability Analysis

In order to ascertain the proposed system's stability, Bode plot analysis is carried out in MATLAB. The plot is given in Fig. 13. The phase margin and gain margin are respectively 47.6^0 and 13.5 dB. Since both the margins are positive, hence it is evident that the PS is stable while in use of this Fuzzy FOTID controller.

TABLE IV. TRANSIENT PERFORMANCE INDICATORS

	Δf_1			Δf_2			ΔP_{tie}		
Controllers	$U_{sh} \times 10^{-3}$ (in Hz)	$O_{sh} \times 10^{-3}$ (in Hz)	T_s (in Seconds)	$U_{sh} \times 10^{-3}$ (in Hz)	$O_{sh} \times 10^{-3}$ (in Hz)	T_s (in Seconds)	$U_{sh} \times 10^{-3}$ (in pu)	$O_{sh} \times 10^{-3}$ (in pu)	T_s (in Seconds)
Fuzzy-FOTID	−20.3374	3.6974	12.1069	−13.3224	3.0573	12.1329	−2.9435	3.0573	4.6521
FOTID	−21.7754	4.1361	15.806	−19.6064	3.4820	16.148	−3.5844	3.4820	6.5585
TID	−24.7216	12.6815	22.9865	−19.3752	12.0934	23.3829	−4.2742	12.0934	6.9576
PID	−23.4279	0.0105	26.2307	−16.2104	0	27.7627	−3.5964	0	20.7197

C. Robustness Analysis

For the purpose of robustness analysis, the controller proposed in this work is subjected to a variation of ±20% for all the parameters used and is depicted in Table V. It is noteworthy to mention that the standard deviation and percentage deviation of the undershoot and overshoot for Δf_1, Δf_2, and ΔP_{tie} is maximum at 1.1331 and 1.59%, respectively, which suggests that the values lie very near to the nominal values for all the parameters. Therefore, it can be concluded that the system performance varies within a miniscule range of standard deviation and percentage deviation which indicates the robustness of fuzzy FOTID controller.

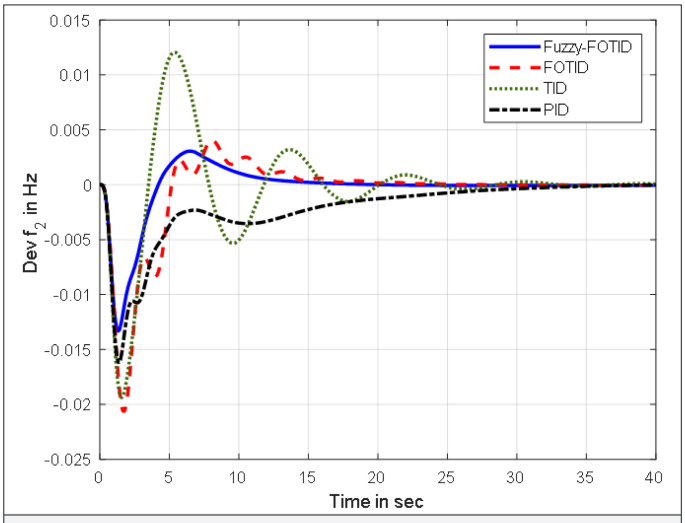

Fig. 11. Area_2 frequency deviation w.r.t time.

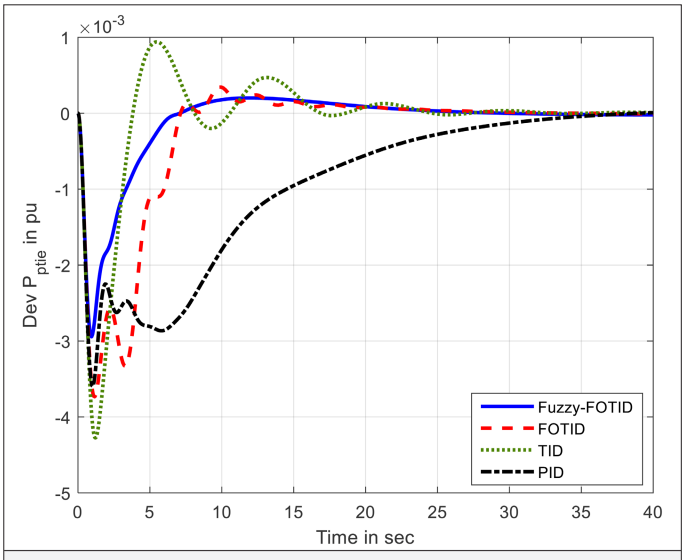

Fig. 12. Tie-line power deviation w.r.t time.

VI. CONCLUSION

The work undertaken here is a first-hand attempt to implement a COA-based Fuzzy FOTID controller for augmenting the frequency stability of a two-area six-unit interconnected PS. The COA tuned said controller is observed to act in a very fast manner in comparison to the other popular controllers as is evident from the comparisons made between their settling time, maximum over and under shoots. It is seen that the fuzzy-FOTID controller exhibits marginal improvement in terms of reduction in overshoot, undershoot and settling time. The proposed controller proves its robustness when it is subjected to variations in all its parameters as well as on the load disturbance, the multi-area system is subjected. The stability study of the system is proved by carrying out the Bode plot analysis. The efficacy of the COA is proved by subjecting it to some standard bench mark functions and then comparing it with SSA and PSO.

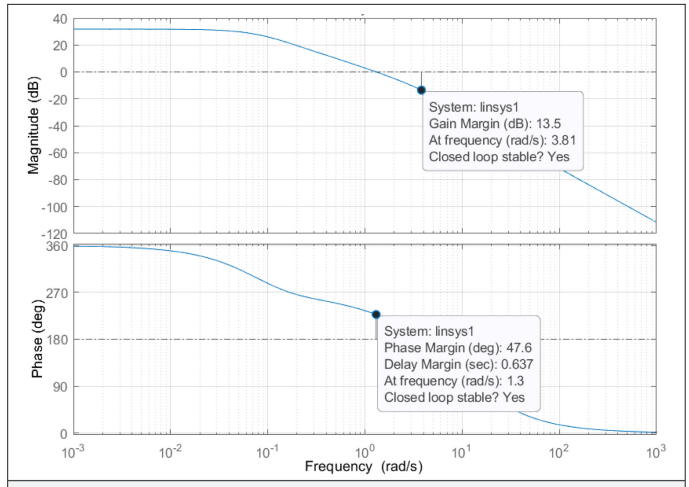

Fig. 13. Bode plot.

TABLE V. ROBUSTNESS ANALYSIS

		Δf_1			Δf_2			ΔP_{tie}		
Parameters	**Variation**	$U_{sh} \times 10^{-3}$ (in Hz)	$O_{sh} \times 10^{-3}$ (in Hz)	T_s (in Seconds)	$U_{sh} \times 10^{-3}$ (in Hz)	$O_{sh} \times 10^{-3}$ (in Hz)	T_s (in Seconds)	$U_{sh} \times 10^{-3}$ (in pu)	$O_{sh} \times 10^{-3}$ (in pu)	T_s (in Seconds)
B	−20%	−21.6268	3.8563	12.89	−16.1321	3.2410	13.1591	−3.2710	3.2410	4.6676
	+20%	−19.5534	3.6999	11.5703	−11.4422	3.0103	11.3921	−2.7334	3.0103	4.6793
R_T	−20%	−20.3717	3.1233	12.6963	−12.9519	2.3720	12.9157	−2.9190	2.3720	4.8794
	+20%	−20.3160	4.1621	11.5507	−13.6036	3.6264	11.4408	−2.9614	3.6264	4.4584
T_G	−20%	−20.0645	3.6212	12.0895	−13.1297	2.9934	12.1073	−2.9206	2.9934	4.6369
	+20%	−20.5696	3.7675	12.1169	−13.5177	3.1206	12.1516	−2.9662	3.1206	4.6629
T_T	−20%	−20.1335	3.5897	12.1540	−12.8492	2.9715	12.1796	−2.8984	2.9715	4.6493
	+20%	−20.6298	3.8239	12.0450	−13.8553	3.1727	12.0756	−3.0069	3.1727	4.6150
K_R	−20%	−20.8700	4.3288	11.7856	−14.6530	3.6417	11.7354	−3.1206	3.6417	4.6136
	+20%	−20.2055	3.2473	12.2726	−12.4249	2.6353	12.3500	−2.8436	2.6353	4.6300
T_R	−20%	−20.3370	3.7356	11.3180	−13.2237	3.0447	11.2934	−2.9294	3.0447	4.5503
	+20%	−20.3381	3.6338	12.8090	−13.3917	3.0327	12.8799	−2.9534	3.0327	4.7350
$K_{PS.}$	−20%	−20.3381	3.6338	12.8090	−13.3917	3.0327	12.8799	−2.9534	3.0327	4.7350
	+20%	−23.1994	4.1862	12.5653	−14.8329	3.3166	12.7144	−3.0241	3.3166	4.7782
T_P	−20%	−23.7560	4.1834	12.6612	−15.0200	3.2756	12.8860	−3.0281	3.2756	4.7911
	+20%	−18.1576	3.7125	11.7094	−12.6212	3.1769	11.6464	−2.9689	3.1769	4.4753
T_{12}	−20%	−20.6481	3.6380	12.1203	−12.0014	2.8326	12.0669	−2.5992	2.8326	4.6862
	+20%	−20.0530	3.8048	12.0989	−14.4754	3.3009	12.1700	−3.2563	3.3009	4.5955
T_W	−20%	−19.8110	3.6342	12.2712	−12.5874	3.0128	12.3170	−2.8438	3.0128	4.6874
	+20%	−20.7419	3.7861	11.9326	−13.9478	3.1228	11.9346	−3.0256	3.1228	4.6042
T_{RS}	−20%	−20.3240	3.8216	12.1451	−13.2196	3.2085	12.1660	−2.9650	3.2085	4.5518
	+20%	−20.3491	3.6500	12.1116	−13.5622	2.9657	12.1545	−2.9359	2.9657	4.8020
Mean		−20.5634	3.7564	12.1693	−13.4925	3.0958	12.2098	−2.9602	3.0958	4.6584
Nominal value		−20.3374	3.6974	12.1069	−13.3224	3.0573	12.1329	−2.9435	3.0573	4.6521
Deviation from nominal value		−1.11%	1.59%	0.51%	−1.27%	1.25%	0.63%	−0.56%	1.25%	0.13%
Standard deviation		1.1331	0.2814	0.4340	1.0672	0.2780	0.5264	0.1452	0.2780	0.1033

Peer-review: Externally peer-reviewed.

Author Contributions: Concept – B.K.S., D.S.; Design – D.S., D.P.D.; Supervision – B.K.S.; Resources – B.K.S., D.S.; Material – B.K.S., D.S., D.P.D.; Data Collection & Process – D.S., D.P.D.; Analysis/Interpretation – B.K.S., D.S.; Literature Survey – D.S., D.P.D.; Writing – D.S., Critical Review – B.K.S., D.S.

Declaration of Interests: The authors have no conflict of interest to declare.

Funding: The authors declared that this study has received no financial support.

REFERENCES

1. O. I. Elgerd, *Electric Energy Systems Theory: An Introduction*, 2nd ed. New Delhi: Tata McGraw Hill, 1982.
2. P. Kundur, *Power System Stability and Control*. 5th reprint ed. New Delhi: Tata McGraw Hill, 2008.
3. B. Dhanasekaran, J. Kaliannan, A. Baskaran, N. Dey, and J. M. R. S. Tavares, "Load frequency control assessment of a P.S.O-P.I.D. Controller for a standalone multi-source power system," *Technologies*, vol. 11, no. 1, p. 22, 2023. [CrossRef]
4. D. K. Gupta, A. V. Jha, B. Appasani, A. Srinivasulu, N. Bizon, and P. Thounthong, "Load frequency control using hybrid intelligent optimization technique for multi-source power systems," *Energies*, vol. 14, no. 6, p. 1581, 2021. [CrossRef]
5. Y. L. Abdel-Magid, and M. A. Abido, "A.G.C. tuning of interconnected reheat thermal systems with particle swarm optimization," 10th IEEE International Conference on Electronics, Circuits and Systems. ICECS 2003. Proceedings of the 2003, Vol.1. Sharjah, United Arab Emirates, 2003, pp. 376–379. [CrossRef]
6. Y. Arya, and N. Kumar, "Design and analysis of BFOA-optimized fuzzy PI/P.I.D. controller for A.G.C. of multi-area traditional/restructured electrical power systems." *Soft Comput.*, vol. 21, no. 21, pp. 6435–6452, 2017. [CrossRef]
7. P. C. Nayak, U. C. Prusty, R. C. Prusty, and A. K. Barisal, *Application of SOS in Fuzzy based P.I.D. Controller for A.G.C. of Multi-Area Power System*. Bhubaneswar, India: Technologies for Smart-City Energy Security and Power (ICSESP), 2018, pp. 1–6. [CrossRef]
8. B. K. Sahu, S. Pati, and S. Panda, "Hybrid differential evolution particle swarm optimisation optimised fuzzy proportional–integral derivative controller for automatic generation control of interconnected power system," *IET Gener. Transm. Distrib.*, vol. 8, no. 11, pp. 1789–1800, 2014. [CrossRef]
9. B. K. Lurie, and United States. National Aeronautics and Space Administration. *Three-parameter tunable tilt-integral-derivative (T.I.D.) controller*. Washington, DC: National Aeronautics and Space Administration.
10. Topno, Pretty Neelam, and Saurabh Chanana. "Automatic generation control using optimally tuned tilt integral derivative controller." In 2016 IEEE First International Conference on Control, Measurement and Instrumentation (CMI), pp. 206-210. IEEE, 2016.
11. S. Priyadarshani, K. R. Subhashini, and J. K. Satapathy, "Pathfinder algorithm optimized fractional order tilt-integral-derivative (FOT.I.D.) controller for automatic generation control of multi-source power system," *Microsyst. Technol.*, vol. 27, no. 1, 23–35, 2021. [CrossRef]
12. Dulău M, Gligor A, Dulău TM. Fractional order controllers versus integer order controllers. *Procedia Engineering*. 2017 Jan 1;181:538-45.
13. Y. Arya, "A novel CFFOPI-FOP.I.D. controller for A.G.C. performance enhancement of single and multi-area electric power systems," *ISA Trans.*, vol. 100, pp. 126–135, 2020. [CrossRef]
14. Y. Arya, "Effect of electric vehicles on load frequency control in interconnected thermal and hydrothermal power systems utilising CF-FOIDF controller," *IET Gener. Transm. Distrib.*, vol. 14, no. 14, pp. 2666–2675, 2020. [CrossRef]
15. Y. Arya, "Impact of ultra-capacitor on automatic generation control of electric energy systems using an optimal FFOID controller," *Int. J. Energy Res.*, vol. 43, no. 14, pp. 8765–8778, 2019. [CrossRef]
16. Babu, Naladi Ram, et al. "Real-time validation of an automatic generation control system considering HPA-ISE with crow search algorithm optimized cascade FOPDN-FOP.I.D.N controller." Archives of Control Sciences (2023): Volume 33 (LXIX), 2023, No.2, 371-390.
17. P. Bhatt, R. Roy, and S. P. Ghoshal, "GA/particle swarm intelligence-based optimization of two specific varieties of controller devices applied to two-area multi-units automatic generation control," *Int. J. Electr. Power Energy Syst.*, vol. 32, no. 4, pp. 299–310, 2010. [CrossRef]
18. B. K. Sahu, S. Pati, P. K. Mohanty, and S. Panda, "Teaching–learning based optimization algorithm based fuzzy-P.I.D. controller for automatic generation control of multi-area power system," *Appl. Soft Comput.*, vol. 27, pp. 240–249, 2015. [CrossRef]
19. S. Z. Mirjalili, S. Mirjalili, S. Saremi, H. Faris, and I. Aljarah"Grasshopper optimization algorithm for multi-objective optimization problems" *Appl. Intell.*, vol. 48, no. 4, 805–820, 2018. [CrossRef]
20. D. Sitikantha, B. K. Sahu, and P. K. Mohanty, "Implementation of WOA based 2DOF-FOP.I.D. controller for A.G.C. of interconnected power system," in *Computational Intelligence in Pattern Recognition*, A. Das, J. Nayak, B. Naik, S. Pati and D. Pelusi, Eds. Singapore: Springer, pp. 909–920, 2020.
21. M. S. Wasim, M. Amjad, S. Habib, M. A. Abbasi, A. R. Bhatti, and S. M. Muyeen, "A critical review and performance comparisons of swarm-based optimization algorithms in maximum power point tracking of photovoltaic systems under partial shading conditions," *Energy Rep.*, vol. 8, pp. 4871–4898, 2022. [CrossRef]
22. M. Dehghani, Z. Montazeri, E. Trojovská, and P. Trojovský, "Coati optimization algorithm: a new bio-inspired metaheuristic algorithm for solving optimization problems." *Knowl. Based Syst.*, vol. 259, p. 110011, 2023. [CrossRef]

Debashis Sitikantha received his bachelor's degree in electrical engineering from Biju Pattnaik University of Technology in 2004, MTech in energy systems and management from ITER, Siksha 'O' Anusandhan (Deemed to be) University in 2012. Presently he is working as an assistant professor in the Department of EEE, ITER, SOA (Deemed to be) University, Bhubaneswar, Odisha, India. He is a member of IEEE. His research interests include automatic generation control, power system protection, industrial automation, embedded systems, soft computing techniques.

Binod Kumar Sahu received his bachelor's degree in electrical engineering from the Institution of Engineers, India, in 2001, his MTech from NIT Warangal in 2003, and PhD from Siksha 'O' Anusandhan (Deemed to be) University in 2016. Presently he is working as Professor in ITER, SOA (Deemed to be) University, Bhubaneswar, Odisha, India. He is a member of IET and IEEE since 2014. His area of research interest includes automatic generation control, fuzzy logic based control, time series forecasting and soft computing techniques.

Debiprasanna Das Completed his BE in electrical engineering in 2004 under Biju Pattnaik University of Technology, in 2004, and his MTech from ITER, Siksha 'O' Anusandhan (Deemed to be) University in 2009. Presently he is an assistant professor at ITER, SOA (Deemed to be) University, Bhubaneswar, Odisha, India. He is a member IEEE. His research interests include electrical machine analysis, automatic generation control, power system, and hybrid electric vehicles.

APPENDIX

$B = 0.4312$ p.u. MW/Hz; $N_1 = 0.8$, $N_2 = -0.2$; $\omega_0 = \pi$;

$R_T = R_H = R_G = 2.4$ Hz/p.u.MW;

$T_G = 0.08$ second; $T_T = 0.3$ second; $T_R = 10$ seconds; $T_P = 11.49$ seconds;

$T_{12} = 0.0433$ MW/rad; $T_W = 1$ second; $T_{RS} = 5$ seconds; $T_R = 28.75$ seconds;

$T_{GH} = 0.2$ second; $K_R = 0.3$; $X_G = 0.6$ second; $Y_G = 1$ second; $c_G = 1$; $b_G = 0.05$;

$T_F = 0.23$ second; $T_{CR} = 0.01$ second; $T_{CD} = 0{:}2$ second;

$a_T = 0{:}543478$; $a_H = 0{:}326084$; $a_G = 0{:}130438$; $a_{12} = -1$